A High-Sensitivity Rapid Acquisition Spectrometer for Lanthanide(III) Luminescence

Patrick R. Nawrocki[1], Villads M. R. Nielsen[1] and Thomas Just Sørensen[1]

[1] Department of Chemistry and NanoScience Centre, University of Copenhagen, Universitetsparken 5, 2100 Copenhagen, Denmark

E-mail: tjs@chem.ku.dk

Abstract

Detecting luminescence beyond 750-800 nm becomes problematic as most conventional detectors are less sensitive in this range, and as simple corrections stops being accurate. Lanthanide luminescence occurs in narrow bands across the spectrum from 350-2000 nm. The most emissive lanthanide(III) ions have bands from 450 nm to 850 nm, some with additional bands in the NIR. Investigating the NIR bands are hard, but the difficulties start already at 700 nm. In general, the photon flux from lanthanide(III) emitters is not great, and the bands beyond 700 nm are very weak, we therefore decided to build a spectrometer based on cameras for microscopy with single-photon detection capabilities. This was found to allieviate all limitations and to allow for fast and efficient recording of luminescence spectra in the range from 450 to 950 nm. The spectrometer characteristics were investigated and the performance was benchmarked against two commercial spectrometers. We conclude that this spectrometer is ideal for investigating lanthanide luminescence, an all other emitters with emission in the target range.

Keywords: Lanthanide(III) luminescence, high resolution optical spectra, luminescence spectroscopy, hardware

1. Introduction

The lanthanide(III) ions are characterized by narrow bands in the optical spectra, and by emission ranging from the ultraviolet to the near-infrared (NIR). While the visible region is characterized by high emission intensities and good instrumentation, spectra including the bands in the NIR suffer from poor data quality.[1, 2] A typical example is the two last bands in the Eu(III) spectrum at 750 nm and 825 nm. These are rarely reported, despite having significant intensities.[3-8] Investigating lanthanide(III) ions that only have emission bands in the NIR are further complicated as their bands are weak in regions where only insensitive instrumention with high noise levels are available. Weak emission in the NIR is due to efficient quenching, a fact with a generalised explanation given by the energy gab law. Thus, the problem of low emission intensity of NIR dyes goes beyond lanthanide luminescence, and efficient characterisation of strong organic NIR emitters is also complicated on standard instrumentation. This is an emerging issue, as emission at longer wavelengths show potential for bioassays and biological imaging suitable for optical applications in both the first (NIR-I, 700 - 950 nm) and second (NIR-II, 1000 - 1700 nm) biological windows.[9-12] These ranges have low absorption attenuation by biological media tissue, and is capable of achieving deep tissue penetration. Efficient characterisation of emitters in these regions is therefore highly relevant.[13-15] Over the last decade, we have looked for commercial suppliers of instruments capable of performing this characterisation. We have been unsuccesful, and now now we have build our own instrument despite reservations regarding the needed calibrations.

We are not the first research group that has been driven to build spectrometers,[16-21] most have, however, been motivated by a specific problems.[22-25] Here, we describe a general spectrometer design, supported by detailed data on samples typical of those we have built the spectrometer to investigate. We are solving a problem we have had in our work, and report a spectrometer design that provide spectra, fast and reliable with little noise, of all the emission lines of europium(III). Further, we show that the performance of the spectrometer is excellent from 450 to 950 nm.

The spectrometer is based on commercial components and is calibrated using NIST traceable standards. To explore the capabilities of the new spectrometer, samples of europium(III) and neodymium(III) solvates in DMSO was chosen. DMSO is a common low-quenching solvent of the lanthanide(III) ions.[26-28] Europium(III) is strongly emissive and is ideal to test the spectrometer in the visible region (580 – 850 nm).[3, 8, 29-33] Neodymium(III) is weakly emissive in the near-IR, and was used to test the NIR-I emission capabilities (880 & 1100 nm).[14, 34-37] The samples were also recorded on two commercial spectrometers for comparison, although only in the 580 – 720 nm range for europium(III). We find that the performance of the spectrometer exceeds that of the commercial instruments, and solves our problem with recording intensity and wavelength calibrated data in the near-IR.

2. Methods and experimental

2.1. Chemicals

Two samples, europium(III) in DMSO and neodymium(III) in DMSO, were measured on all the listed instruments. All chemicals were used as received. To make 50 mM lanthanide(III) DMSO solutions, 89.88 ± 0.2 mg $Eu(CF_3SO_3)_3$ (98 %, Strem Chemicals) or 88.72 ± 0.2 mg $Nd(CF_3SO_3)_3$ (> 97.0 %, TCI Chemicals) were dissolved in 3 mL DMSO (HPLC grade, VWR).

2.2. Optical Spectroscopy

All experiments have been measured at room temperature and in 10 mm quartz cuvettes (23/Q/10) from Starna Scientific.

Cary Eclipse – Agilent Technologies

Steady-state emission spectra were recorded on the Cary Eclipse spectrometer, with the dedicated hardware using the pulsed xenon arc lamp and the single-channel photomultiplier tube detector on medium bias setting. Emission spectra were recorded using a 395 nm excitation wavelength. Excitation slits were set to 20.0 nm, emission slits to 5.0 nm, a data interval of 0.5 nm and a 1.0 second integration time. Excitation and emission filters were kept open. The spectra are assumed to be corrected before they are outputted.

PTI QuantaMaster 8075-22-C – HORIBA Scientific

Measurements on the PTI spectrometer were performed using the dedicated hardware in steady state mode, with a xenon arc lamp as excitation source and a single-channel photomultiplier tube detector in the visible (Hamamatsu R13456) and a liquid nitrogen cooled InGaAs PIN photodiode in the NIR range (HORIBA Scientific DSS-IGA020L). Emission spectra were recorded using 395 nm excitation wavelength. Excitation slits were set to 8.0 nm, emission slits to 0.5 nm in the visible range and 1, 4 and 8 nm in the NIR region. A data interval of 0.2 nm and a 1.0 second integration time were used. The spectra are corrected using a reference detector to monitor excitation source fluctuations. The spectra are further manually background corrected as the dedicated software does it wrong.

Cary 5000 Absorption Spectrometer – Agilent Technologies

Absorption spectra were performed to provide supporting data and to verify sample purity. They were performed on the Cary 5000 double beam absorption spectrometer. The measurements were recorded in the 270 – 600 nm range for europium(III) and the 270 – 950 nm range for neodymium(III). Integration time was set to 0.2 seconds, data interval to 0.2 nm, and width to 0.5 nm. A lamp change is set to occur at 350 nm, a second combined detector and grating change occur at 835 nm. For each measurement, the instrument baseline was determined for the empty cuvette. Ideally, the baseline should be for the solvent, in order to determine the absolute absorption for the sample, but we decided to record the pure DMSO spectrum. The absorption data presented herein was recorded as part of a larger sample series with changing solvent. In this case, baselining against an empty cuvette is less prone to human error, albeit less precise. This was then manually subtracted from the sample absorption spectra to obtain the sample absorption. The optical window for lanthanide(III) triflates in DMSO stops at 350 nm. Data below this wavelength should not be considered.

Custom Spectrometer – SuCo

Like the commercial spectrometers, the custom spectrometer consist of an excitation source, a detection system, and control software. In addition, the construction elements are detailed.

Support and construction: The spectrometer is built on a 140 kg table with a 1500x1500 mm table top with shelving underneath for the supercontinuum laser, desktop computer etc. The table supports 250 kg per 1 m^2. On the table top two 1500x750x65 mm 70 kg M6 breadboards were combined using a 150x150x12 mm and a 200x200x12 mm breadboard. The assembly is free floating.

Power, computer, and connectors: The table is fitted with a two 6 socket power strip from a single group providing a 220 V/50 Hz with a maximum load of 13 A. The components are supplied with both connectors and power supply. A desktop computer in a cabinet with at least 8 USB slots are required and two Ethernet ports for dual-detector setups. Keyboard, mouse, and a minimum 19" HD monitor is recommended. Internet access is not needed.

Excitation system: A supercontinuum laser (NKT SuperK Fianium FIU-15) coupled with a tuneable band pass filter (NKT LLTF Contrast VIS/SWIR HP8) was used as the excitation source. The system provides efficient excitation selection in the wavelength range 450 – 1900 nm, with a bandwidth of 2.5 nm (visible) and 5 nm (SWIR), a step-size of 0.05 ± 0.02 nm, and a power over the entire range of no less than15 mW/cm^2 at 500 nm and a rapid decline towards shorter wavelengths. Beam size is approximately 3 mm^2. The output of the LLTF is a collimated, single wavelength, pulsed beam and post-mounted irises (Thorlabs SM2D25) are the only elements required to clean the excitation light.

Sample compartment: The sample compartment was constructed from black polymer board and aluminium supports. The sample compartment measures 650x400x300 mm and the lid includes a 155 mm opening that allows the use of cryostats.

A wedged optical laser window (Thorlabs WW11050) was placed after the iris for laser power monitoring using a Si photodiode power meter (Thorlabs PM16-130).

A temperature controlled sample holder with dry flush and magnetic stirrer (Luma 40/FS5) is mounted on a 100x150x12 mm raised breadboard for height adjustment to 145 mm to match the illuminated volume with the entrance slit of the detection system. The sample holder is for standard cuvettes with a 10x12 mm rectangular opening on all four sides.

A NIST traceable lamp (StellarNet Inc. SL1-CAL halogen source lamp) is mounted facing the detector system through the sample holder.

Detection system: An optical lens with focal length = 80 mm (Thorlabs AC508-080-AB) is used to create an image of the illuminated volume in the sample holder. The image is created on the entrance slit of a 500 mm Teledyne Princeton Instruments (TPI) polychromator (TPI SpectroPro HRS-500). Just in front of the entrance slit a post-mounted filter wheel (Thorlabs FW1A) with long pass filters (Thorlabs FELH0500, FEL0800) is placed. In front of the filter wheel a post-mounted iris (Thorlabs SM2D25) is placed.

The polychromator is fitted with a three interchangeable gratings that disperse the light on the detector.

The detector is a liquid nitrogen cooled CCD camera (TPI PyLoN 400B-eXcelon) with a 1340 x 400 pixel array chip with a total size of 26.6 x 8 mm. The operational temperature is -120 °C, maintained by the liquid nitrogen in the 2.7 L reservoir. The detector has an operational range of 325 – 1050 nm defined by a 5 % quantum efficiency (QE) limit.

Control software: The supercontinuum laser is operated by the Control software distribution by NKT Photonics, and allow the laser power (0 – 100 %) in 0.1 % increments and pulse repetition rate (0.15 – 78 MHz).

The LLTF Contrast operates via the PHySpec software developed and distributed by Photon etc., controlling the tunable bandpass from 450 – 1900 nm. With PHySpec, macro functions allow wavelength variation to be automated at set time intervals. Internal gratings on the LLTF Contrast are set to automatically change at 775 nm.

All TPI products can be controlled with the Lightfield software. The hardware is automatically registered by the software and the spectrometer is assembled virtually in the software by dragging and dropping the components into the desired connectors. Only a single detector can be connected to the spectrograph via Lightfield at any given time. Once registered, all functions from the connected hardware are grouped into collapsible tabs for easy organization. Gratings can be selected from a dropdown menu, and an input for a central wavelength is required to orient the grating turret to generate a spectrum at ± 100 nm from the input wavelength. A flip mirror can be engaged to redirect the dispersed light to the secondary exit port. Rotational and longitudinal alignment has been performed via the Experiment Menu, wavelength calibration of each grating via the Calibration tab with a simplified setup using the IntelliCal (TPI IntelliCal) calibration lamp for grating-wide calibration. Spectra are collected in spectrometer mode, integrating pixel columns into a single data point for rapid spectrum acquisition. Measurements are output as Lightfield compatible .spe image formats, and are exported as .csv files. Exposure times are given in millisecond by default and

background measurements are acquired at 5 times the exposure time by default. Any .spe file can be used in place of a background measurement. Cosmic ray filtering is engaged and averaging of multiple exposures per frame, i.e. multiple measurements per single spectrum, is typically used to improve signal-to-noise ratios.

All components of the custom spectrometer are illustrated in the schematic in Figure 1 and the choice of components is discussed in detail below. The measurements indicated in Figure 1, and the details provided above will allow for the construction of an identical spectrometer. A full list of components used in each assembly, and a full bill of materials can be found in the supporting information.

The polychromator uses a grating to disperse the light in the detection system. In this system, the polychromator is fitted with a turret with three gratings. The specifications of these are:

1. 500 nm blaze, 300 g/mm, 330 – 880 nm optimum range, mechanical scan range 0 – 6 µm, 68x68 mm (TPI i1-030-500-P)
2. 750 nm blaze, 300 g/mm, 500 – 1200 nm optimum range, mechanical scan range 0 – 6 µm, 68x68 mm (TPI i1-030-750-P)
3. 1200 nm blaze, 300 g/mm, 700 – 2100nm optimum range, mechanical scan range 0 – 6 µm, 68x68 mm (TPI i1-030-1200-P)

Settings used to investigate laser power dependencies. Laser power experiment was done using an excitation wavelength of 580 nm exciting a sample of 50 mM neodymium(III) DMSO. An 800 nm long pass filter was used, a 25 µm emission slit and the 750 B grating oriented at a 880 nm center wavelength. Exposure time was set to 1000 ms without averaging of multiple exposures. By acquiring a measurement with the chosen settings and the laser turned off, a .spe file was generated and used as input file for background subtraction. Laser power was changed by increments of 5 % from 0 – 100 %.

Settings used to investigate the effect of increased exposure time. Exposure time experiment was done using an excitation wavelength of 580 nm at 90 % laser power exciting a sample of 50 mM neodymium(III) DMSO. An 800 nm long pass filter was used, a 25 µm emission slit and the 750 B grating oriented at a 880 nm center wavelength. By acquiring a measurement with the chosen settings and the laser turned off, a .spe file was generated and used as input file for background subtraction. Exposure times were changed by increments of 1 ms from 1 – 10, of 5 ms from 10 – 25, of 25 ms from 25 to 200 and at larger even larger increments above this threshold as indicated in Figure 2b.

Experiment used to investigate slit width dependencies. Slit width experiment was done using an excitation wavelength of 465 nm at 90 % laser power exciting a sample of 50 mM europium(III) DOTA. A 500 nm long pass filter was used and the 750 B grating oriented at a 640 nm center wavelength. An exposure time of 1000 ms was used and averaging 10 exposures per frame. By acquiring a measurement with the chosen settings and the laser turned off, a .spe file was generated and used as input file for background subtraction. Slit size was varied by increments of 1 µm from 1 – 5, and of 5 µm from 5 – 70.

Settings used and operational steps required to record emission spectra. Based on the results of the mechanical parameters listed above, the measurements of samples of 50 mM europium(III) and neodymium(III) DMSO was measured accordingly.

Laser power is set to 90 % and maximum (78 MHz) repetition rates in the Control software. The excitation wavelength is chosen with the PHySpec software, 465 nm for europium(III) and 580 nm for neodymium(III). Long pass filters were manually changed to 500 nm for europium(III) and 800 nm for neodymium(III), and the emission slit set to 25 µm for all measurements.

In the Lightfield software the 750 B grating was selected and center wavelengths of 660 nm and 880 nm were chosen for europium(III) and neodymium(III), respectively. All acquisitions used different exposure times and exposures per frame, as listed in the legends of Figure 4-6. By acquiring a measurement with the chosen settings and the laser turned off, a .spe file was generated and used as input file for background subtraction.

2.3. Intensity calibration

The detection efficiency of the detector system was calibrated using the response of a NIST-calibrated lamp from StellerNet Inc. (SL1-CAL halogen source lamp, S/N 222541). The true spectrum is convoluted by the product of the efficiency of all optical components in the detection system of the spectrometer. The measured spectrum must therefore be corrected by the quantum efficiency of the detection system, $QE_{detection\ system}$.

$$I^{\lambda}_{measured} = I^{\lambda}_{TRUE} \cdot QE^{\lambda}_{detection\ system} \qquad \text{Eq. 1}$$

$$I^{\lambda}_{TRUE} = \frac{I^{\lambda}_{Ln}\ measured}{QE^{\lambda}_{detection\ system}} \qquad \text{Eq. 2}$$

$QE_{detection\ system}$ is obtained by recording a spectrum of the NIST-calibrated lamp, I_{NIST}, and correcting with the provided NIST traceable lamp spectrum $I_{NIST.TRUE}$.

$$I^{\lambda}_{NIST} = I^{\lambda}_{NIST,TRUE} \cdot QE^{\lambda}_{detection\ system} \quad \text{Eq. 3}$$

$$QE^{\lambda}_{detection\ system} = \frac{I^{\lambda}_{NIST}}{I^{\lambda}_{NIST,TRUE}} \qquad \text{Eq. 4}$$

The $QE_{detection\ system}$ obtained from Eq. 4 is the correction file needed to correct the measured spectrum and obtain the true intensity corrected emission profile according to Eq. 2. Note that all the parameters above are wavelength dependent. Further, $QE_{detection\ system}$ depends on all the elements in the detection system. Any change in the detection system requires a new calibration and a new correction file. The variables in the detection system are; excitation beam position on the excitation side, lenses, lens positions, irises (open/closed only as there is no control on iris size), filters inside the sample compartment, grating, grating position (center wavelength), detector temperature, and detector binning on the emission side.

If any of these are changed a new correction file must be created. For this reason, a NIST traceable lamp has been included as part of the spectrometer.

3. Results & Discussion

3.1. Spectrometer Components

The instrument has been built with modular components from multiple vendors to achieve a spectrometer with high sensitivity in the spectral range from 450—850 nm. Here, the selection of the components will be described in context of their function in the spectrometer. Figure 1 shows a layout of the spectrometer, including the detailed specifications of the sample compartment. The description of the components follows the ligth through the spectrometer.

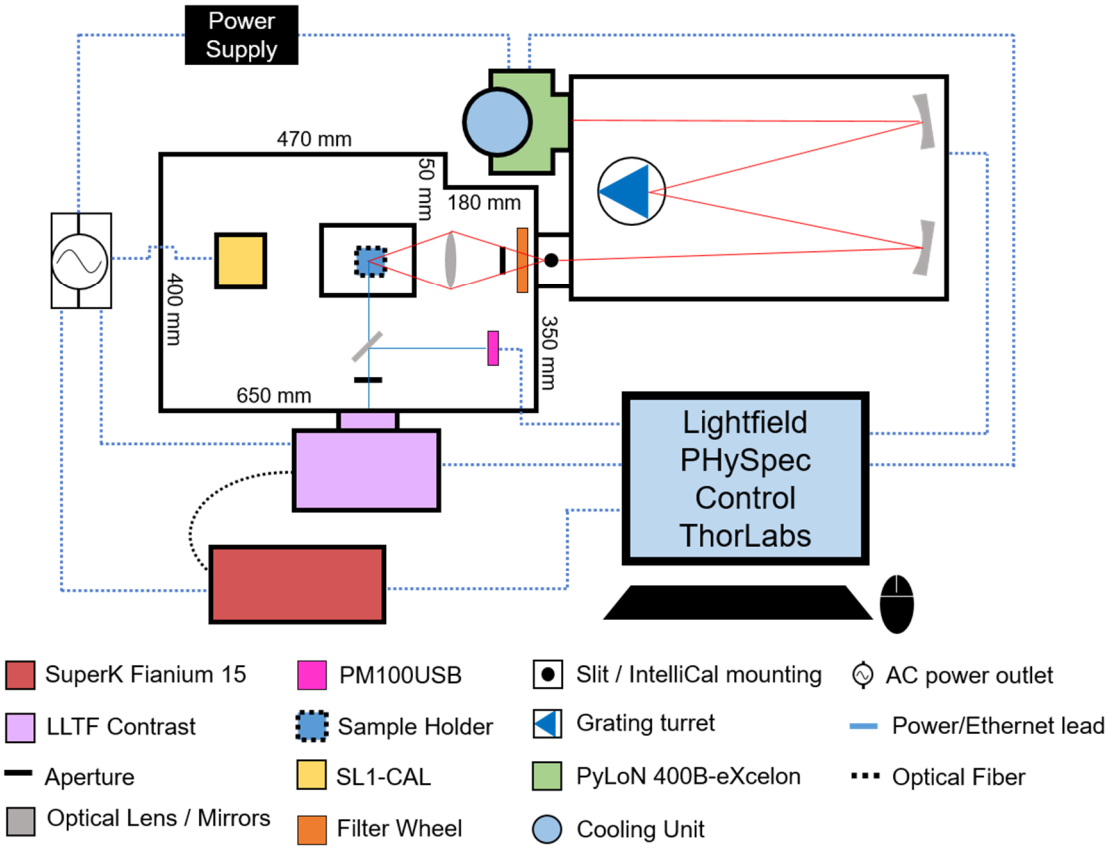

Figure 1 – Top-down view of the custom spectrometer and the schematic diagram describing the setup components. Purge tubes and temperature wires for SL1-CAL and Luma 40/FS5 are omitted in the picture. Sample compartment dimensions are in mm.

Excitation Source The excitation source consists of the SuperK Fianium 15 pulsed white light supercontinuum laser that in combination with the LLTF Contrast produce a tunable, high-powered broadband excitation source. The excitation source provides 2.5 nm (visible) or 5 nm (NIR) wide excitation tunable beam in steps of 0.5 ± 0.02 nm in the range from 450 — 1900 nm. The 15 W/cm^2 minimum power allows for direct excitation in the low molar absorption coefficient bands of the lanthanide(III) ions, and the use of highly dilute samples of brigther chromophores.

Sample Compartment The sample compartment consist of a custom-built black box. Stray light is observed from the excitation beam from the LLTF. This is removed with an iris. The sample holder was chosen for standard issue 10 mm cuvettes. With temperature control and gas purging, temperature effects are readily studied. With magnetic stirring, *in-situ* experiments can be performed. Note that dynamics on millisecond timescales can be probed by using the combination of high excitation power and a sensitive detection system with short readout time. The sample holder is placed 320 mm from the detector system entry slit. Along the path to the detector system a 80 mm focal length achromatic doublet optical lens placed at 160 mm. The lens is mounted in a clip-on mount that is to be changed between the current visible optics and NIR optics. Just before the detector system entry slit, we placed a 5-position filter wheel with long pass filters. The filters are used to remove scattered excitation light.

A NIST traceable lamp from the SL1-CAL is used for characterizing the overall QE of the detector system. It is needed in order to provide the correction files needed to compensate for imperfections in the detector system. The calibration lamp is placed on the other side of the sample holder 380 mm from the detector system entrance slit. The high intensity of the intensity calibration lamp saturates the sensitive detector system. The solution is an iris that is placed in front of the filter wheel.

The IntelliCal, a switchable Hg/NeAr wavelength calibration lamp from Teledyne Princeton Instrument, can be mounted in front of the entrance slit.

The sample compartment is large and completely customizable, which allows for solid state setups, entrance/exit polarizers, and cryostats etc. to be mounted.

Detector System The detector system starts at a manually operated slit. The excitation volume is via the lens imaged on the slit. Note, that the light is not focused onto the slit. The sensitivity of the detector system, and the power of the excitation source, makes focusing unnecessary.

The physical slit width is measured in µm, which is translated to sub-nm spectral resolution on the CCD detector. The resolution is readily documented by mounting the wavelength calibration lamp. Calibrating the wavelength axis provides a spectral resolution of 0.2 ± 0.05 nm using a 5 µm slit.

The slit is the entry point for a SpectroPro HRS-500 polychromator with a focal length of 500 mm. The light is collected by a toroid mirror and focused on a turret with a diffraction. The gratings ability to disperse light is depending on the number of grooves per unit area, g/mm, and the grating efficiency as a function of wavelength is described by the central wavelength of the grating. The grating turret holds three gratings, and the detector system is equipped with three 300 g/mm gratings, blazed at 500 nm, 750 nm and 1200 nm. The grating turret is readily replaced.

The grating disperses the focused light, resolving the individual energy components in space. The first order diffraction is collected by a second toroidal mirror and focused on one of the two detector ports. A flip mirror selects which detector port that is active.

The detector is a PyLoN 400B-eXcelon 1340 x 400 pixel CCD camera with an operational range of 325–1050 nm (threshold: QE ≥ 5 %). The detector is cooled to -120C to achieve single photon detection. The detector system is used for spectroscopic application. The resolution is therefore only required in one of the detector axes, as only the energy axis resolved along the 1340 pixels on the x-axis has great significance. The CCD chip layout allows vertical binning, which in turn allows for a readout speed of 60 spectra per second. In imaging mode, where all pixels are read out individually, only 6 spectra can be recorded per second. These framerates are theoretical values that changes depending on exposure time and chip readout kinetics. The detector can handle integration times down to 1 ms, but only 60 spectra can be readout per second at full resolution. If only parts of the chip is read, or if horizontal binning is used (lowers resolution), spectra can be recorded even faster.

The combination of 300 g/mm gratings, 500 mm focal length, and the 26.8 mm wide CCD chips provides a 200 nm spectral width. That is each measurement provides a 200 nm spectral window recorded across 1340 pixels, which translates to a ~0.15 nm data point spacing. The narrow width and high resolution was chosen with lanthanide luminescence in mind. A lower grow density, a higher spectral width, would be an advantage for organic emitters. Yet, with the very fast data collection and internal intensity calibration, wider spectral ranges are readily obtained by combining data obtained in different ranges e.g. from two or more measurements.

Software The setup uses multiple pieces of software to handle different parts of the hardware.

The SuperK Fianium 15 can be controlled via the Control software from NKT Photonics. This software configures laser power and repetition rates. This can also be done manually on the laser panel.

The LLTF Contrast can be controlled on the PHySpec software, developed and distributed by Photon etc. With this software, the excitation wavelength is selected. Semi-automation can be created with the built in macro functions.

All Teledyne Princeton Instruments hardware (SpectroPro HRS-500, PyLoN 400B-eXcelon, IntelliCal) are operated from the Lightfield software from Teledyne Princeton Instruments. All functions, with the exception of the slit width, can be controlled via the software instances.

3.2. Spectrometer Characterization

The custom spectrometer differs in layout from traditional luminescence spectrometers, and we start by characterising the available variables: Laser power, integration time, and slit width. These variables change the observed signal intensity. In addition, the slit width also dictates the spectral resolution. Note that the grating dictates the data point density, which with a 300 g/mm grating is ~0.15 nm. The slit width controls both spectral resolution and signal intensity, both set of data are analysed. The data is shown in Figure 2, all experimental data can be found in the Supporting Information. The dependence of signal intensity on laser power, integration time, and slit width was investigated using a sample of neodymium(III) in DMSO. The signal used is the 880 nm band, and the signal plotted in figure 2 is the area of the band. In figure 2, the effect of slit width was investigated using europium(III)

luminescence. The europium(III) line at 580 nm in the $[Eu.DOTA]^-$ complex approximates a line shape, which enabled the experimental evaluation of the spectral resolution.

First, the luminescence signal as a function of laser power setting (Scale: 0 – 100 %) was recorded. The results is shown in Figure 2a. The luminescence signal shows good linearity of power above 50 %. Below 50 %, the luminescence signal enters a non-linear regime, and below 30 %, barely any intensity can be observed. The data points represent integrated emission areas, and error bars for each point are generated from the sum of collected photons, $1/\sqrt{N}$, and the reported laser stability (± 0.5 % reported). A linear fit of the data points above 50 % has an R^2 value of 0.9944. Despite this R^2 value, some variation is seen in the data points. The precision of the data points are a convolution of background variation and laser stability, but based on the plotted errors, these factors do not explain the variation. Similar behaviour is observed for other samples, including fluorescein and Ludox, which are provided in Figures S8-S10 at various wavelengths. We conclude that all measurements should be recorded at laser powers above the 50 % threshold where laser performance is reliable. All further measurements were performed with 90 % laser power.

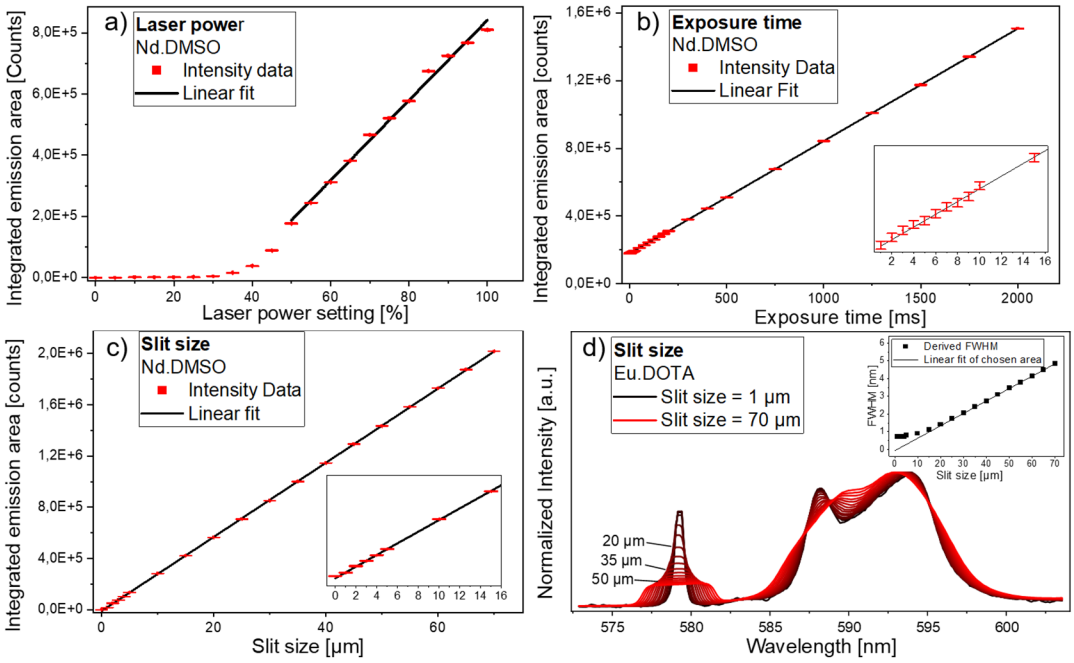

Figure 2 – Physical parameters of the custom spectrometer. Variation in the emission intensity of the 880 nm band of 50 mM neodymium(III) in DMSO is used to characterize a) laser power output, b) exposure time and c) slit width, and d) Effect of slit width on the spectral resolution of the 580 nm spectral line and the 590 nm band in 50 mM europium(III) DOTA in aqueous solution. Insert show the derived FWHM values of the 580 nm line. Errors bars are shown in all plots but are too small to see. Europium(III) centred data and neodymium(III) centred data was collected while using an excitation wavelengths of 465 nm and 580 nm, respectively.

The integration time was presumed to change the luminescence signal with a linear increase as a function of integration time. The data in Figure 2b confirms this assumption, but the y-intercept of a linear fit reveals that the intensity does not go to zero. This is most likely due to the lack of a shutter in the system, as the Pylon detector is known to be sensitive to light exposures between measurements. We will report further on this in later reports, where we are using the spectrometer.

Finally, the effect of the slit width on luminescence signal intensity was considered. Here, the intensity also follow linear behaviour, see Figure 2c.

A separate investigation of how the slit width effects the spectral resolution is seen in Figure 2d. The theoretical limit is ~0.2 nm with the current gratings. We use the 580 nm line of europium(III) ($^5D_0 \rightarrow {}^7F_0$ transition) to determine spectral resolution. The spectral profile of this line in solution should be that of a Gaussian function. Figure 2d shows

the line change as a function of slit width. The data shows that up to a slit width of 10 µm, we resolve spectral information. Slit widths between 10 µm and 35 µm still contains some spectral information, while we at slit widths above 35 µm only see the image of the slit. Note that these considerations are only relevant in lanthanide luminescence, as the much wider bands of organic chromophores rarely will show this kind of effects when the spectral resolution is below 3 nm (50 µm)

At slit widths below 10 µm, the 580 nm europium(III) luminescence line is recovered as Gaussian function with a width of 0.62 ± 0.01 nm. Thus, the spectral line is ~3 times the theoretical limit, and verifies that the spectral information is not limited by the instrument. As the spectral resolution increase at higher wavelengths, we can conclude that the spectrometer is ideally suited to record for lanthanide(III) spectra. We note that higher spectral resolution will be needed for solid and cryogenic samples, which can be achieved by substituting the 300 g/mm gratings for e.g. 600 g/mm or 1200 g/mm. This reduced the spectral window, but increases spectral resolutions. Similarly, grating with a lower groove density can be used if only organic dyes are to be investigated.

3.3. Spectrometer Calibration

The emission intensity calibration follows the procedure described from Eq. 1-4., wavelength dependant $QE_{detection\ system}$ from Eq. 4 is obtained to correct measured spectra to obtain I_{TRUE}. The factory provided correction file, shown in Figure 3a, represent the "true" spectral profile of the NIST-traceable SL1-CAL lamp, independent of instrumentation. Comparing the SL1-CAL factory profile, $I_{NIST,TRUE}$, with the SL1-CAL measured on the custom spectrometer, I_{NIST} Figure 3b, illustrate the convolution of the SL1-CAL and the detection system, $I_{NIST} \cdot QE_{detection\ system}$. The measured SL1-CAL response is divided by the factory provided response profile to generate the $QE_{detection\ system}$.

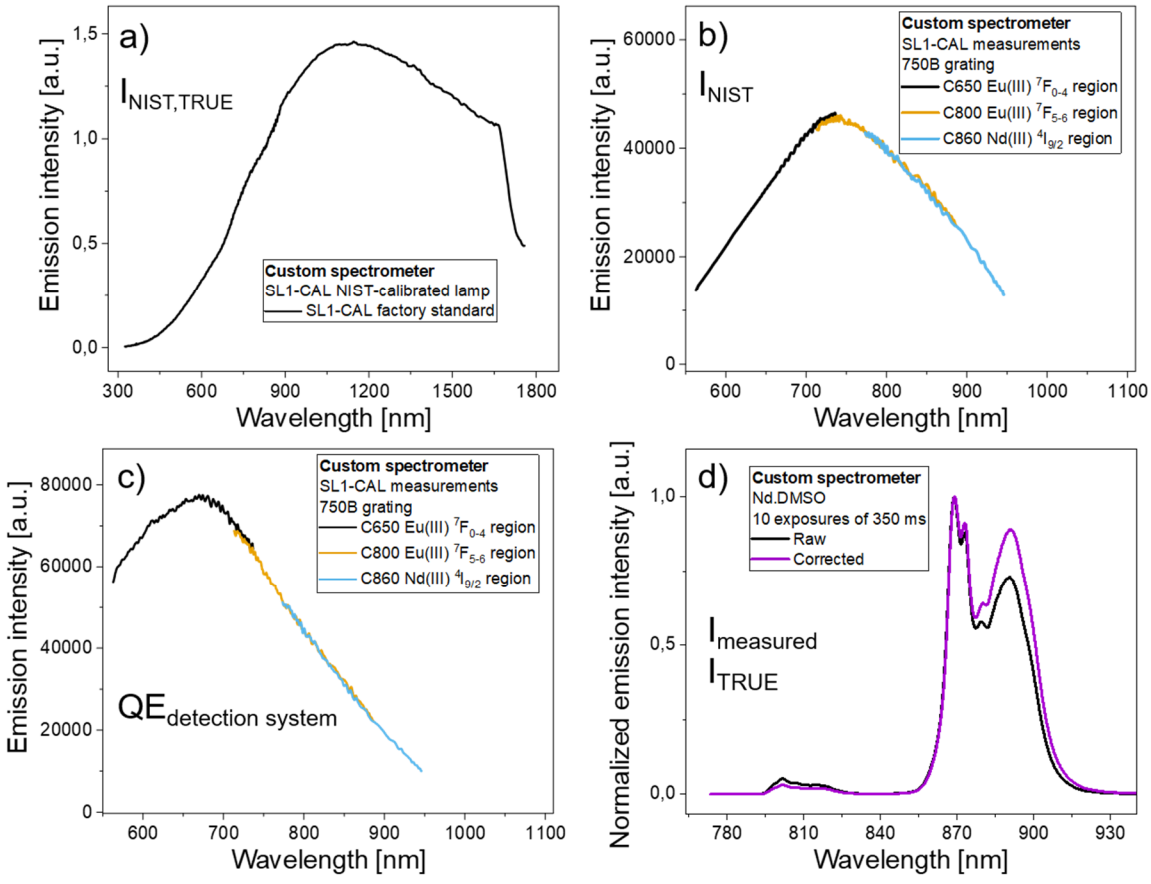

Figure 3 – Steps of the spectrometer intensity calibration. a) Factory provided profile of the NIST-traceable SL1-CAL lamp b) Response of the SL1-CAL lamp measured on the 750 B grating on the custom spectrometer. Each curve is measured at a specific

centre wavelength on the grating c) Calibration curves of the detector system generated by correcting the measured SL1-CAL response by the factory provided profile of the SL1-CAL d) Relative intensity differences of a neodymium(III) DMSO spectrum before and after correction of the C860 calibration curve.

Using $QE_{detection\ system}$, data recorded on the custom spectrometer, $I_{measured}$, can be corrected to obtain I_{TRUE}. In Figure 3d, the normalized profiles of $I_{measured}$ and I_{TRUE} are plotted against each other to show the differences in relative intensities. From the comparison, it is seen how the $I_{measured}$ spectrum show marked relative intensity differences of the peaks at 870 nm and 890 nm, while in the I_{TRUE} spectrum, these peaks are equally intense.

3.4. VIS/NIR-I Performance

With the custom spectrometer variables characterised and the spectrometer calibrated, we turn to the performance of the new instrument. Measurements were performed to compare the custom instrument to two commercial spectrometers. The entry-level Cary Eclipse from Agilent Technologies and the state-of-the-art PTI QuantaMaster 8075-22-C from Horiba Scientific. Samples of 50 mM europium(III) or 50 mM neodymium(III) in DMSO were measured. These lanthanides are chosen as their emission intimately known,[29, 38-40] and as they allow the capabilities of the spectrometer to be assessed beyond 700 nm, to the 950 nm benchmark that was targeted.

The comparison is performed in a manner that should provide comparable data quality. Every data point is collected with a 1 second integration time. The Cary Eclipse and PTI QuantaMaster instruments have single channel detectors and scanning monochromators, and the spectra from these are constructed by scanning the emission wavelength. A spectrum with a 1 second integration time and a data point spacing of 0.15 nm across a 200 nm spectral window takes 1333 seconds (~20 minutes) to record. In contrast, the custom spectrometer records the entire spectrum in 1 second.

When considering the comparison, it should be noted that the Cary Eclipse uses a pulsed xenon lamp and a detector where the amplification voltage can be adjusted from 200 V to 1000 V. The nominal detection window is up to 900 nm. It should be noted that the PTI QuantaMaster uses Xe arc lamp excitation source and is equipped with dedicated vis and liquid nitrogen cooled NIR detectors, with a nominal detection window beyond 1200 nm. The custom spectrometer uses a pulsed white light laser as excitation source, and has an array detector with a nominal detection window up to 1050 nm.

Spectrometer Comparison The raw data recorded across the three spectrometers are shown in Figure 4. Note that Figure 4 reports raw, uncalibrated data and the spectra is a convolution of luminescence signal and detector system quantum efficiency. Therefore, the relative peak intensities are meaningless, and we focus on data quality (signal-to-noise) and spectral resolution only. Cursory inspection of Figure 4 reveals that the intense europium(III) bands are detected by all the spectrometers, while the 880 nm neodymium(III) luminescence band is only observed by the custom spectrometer.

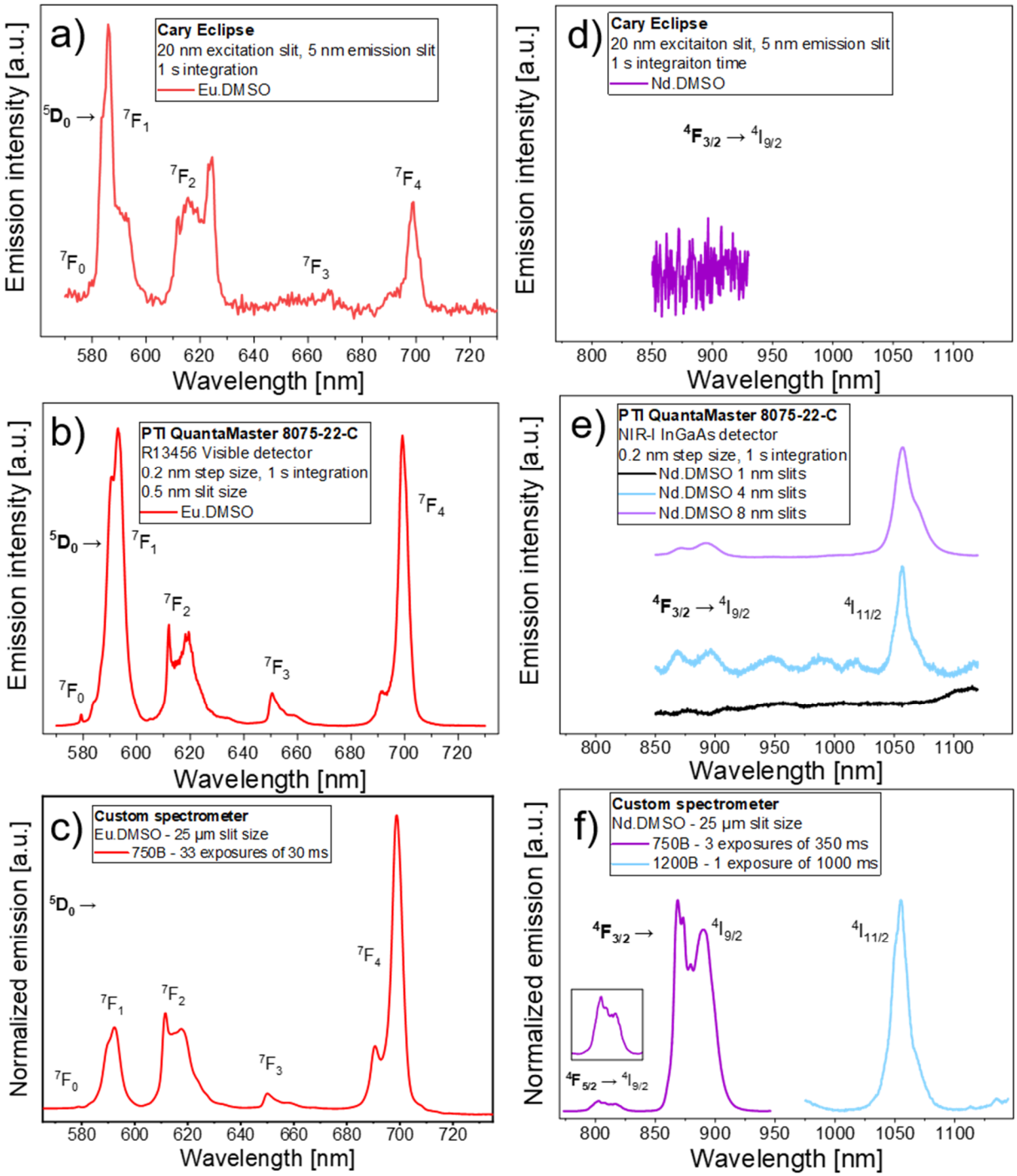

Figure 4 – Spectrometer comparisons from emission spectra of 50 mM concentrations of europium(III) (a-c) or neodymium(III) (d-f) solvates in DMSO. All measurements are made so that the integration time per data point equals 1 second. The europium(III) and neodymium(III) spectra were recorded with excitation wavelengths of 465 nm and 580 nm, respectively.

Considering the data in Figure 4 in more detail the europium(III) spectrum is readily recorded on the Cary Eclipse at the instruments high-performance settings, but even at this setting the data quality is inferior to the other two instruments. Between the PTI QuantaMaster and custom instrument, the data quality and resolution are comparable with the PTI QuantaMaster yielding a higher level of noise. The difference is particularly evident in the 615 nm band. When comparing these spectra, the integration times of 1 second data becomes important. The entire spectrum in

Figure 4c is recorded in a single second on the custom spectrometer. The spectrum in Figure 4b from the PTI QuantaMaster required 800 seconds or a little over 13 minutes. This clearly illustrates the power of the custom spectrometer.

The neodymium(III) DMSO samples provide similar information, although the Car Eclipse for all practical purposes must be considered to be limited to a detection window below 800 nm. The PTI QuantaMaster and the custom instrument deliver similar quality data in the region up to 700 nm, disregarding the acquisition time. In the NIR, the PTI QuantaMaster does not perform up to the same standard. If the parameters are changed, and 8 nm emission slits are used, the 880 nm emission band can be differentiated from the background. The spectra from the custom instrument clearly illustrate the fine structure that is lost by going to 8 nm slits. This is information cannot be recovered by the PTI QuantaMaster. In contrast, even luminescence from a thermally populated higher lying energy level of neodymium(III) are observed when using the custom spectrometer. The spectrometer is clearly delivering the performance it was design to do.

Custom Spectrometer Capabilities – Europium(III) and Neodymium(III) luminescence With the performance of the custom setup established, we can now take a closer look at the capabilities of the new instrument. The spectrum of europium(III) in DMSO is shown in Figure 5. The inserts in Figure 5 are normalised, intensity, integration time, and wavelength corrected, and the relative intensities are considered true. The intensity and wavelength correction are performed as described above, and the integration time is corrected using the function shown in Figure 2b. The slit width is 25 μm, thus, the broad bands arise from the weighted averages of several species in solution.[41-44] It should be noted that the europium(III) spectrum now includes high quality data for the 750 nm and 810 nm bands that provide information on the fine structure. These bands are often omitted, and we have previously been unable to produce a data quality on the PTI QuantaMaster that was suitable for extracting information from these bands.[3]

The neodymium(III) spectrum, shown in Figure 6, shows the current limits of the set-up. While the low intensity band at 880 nm is well resolved, and provided able information through the recovered fine structure, the calibration routine fails for the 1060 nm band. We are changing gratings, moving into a spectral region were the detector performance is poor,[1] and using very long integration times. If we are to succeed in extending the range of the custom spectrometer beyond 950 nm, more work is required on both the instrument and the calibration procedures. We do note that fine structure is resolved in the 1060 nm band, which exceeded our expectation due to the poor detector efficiency at this wavelength. We were further surprised, as we could measure a fine structured band corresponding to luminescence from the thermally populated $^4F_{5/2}$ level. This is to the best of our knowledge, the first time this band is reported for a neodymium(III) complex in solution.

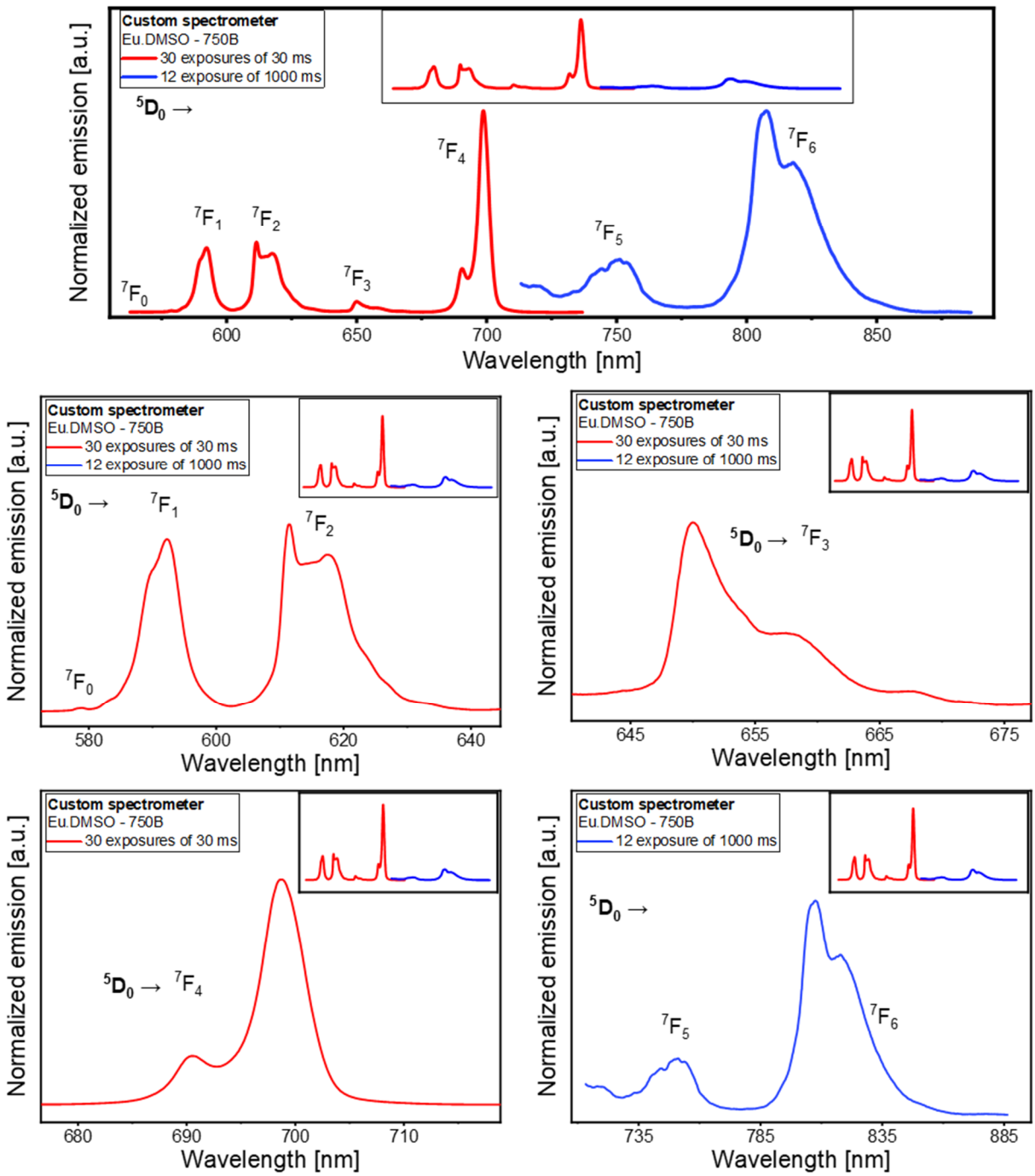

Figure 5 – Emission spectra of 50 mM europium(III) in DMSO recorded on the custom spectrometer using an excitation wavelength of 465 nm. Exposure times and number of exposures per measurements changed to optimize for good signal-to-noise ratios. Inserts show intensity corrected emission spectra.

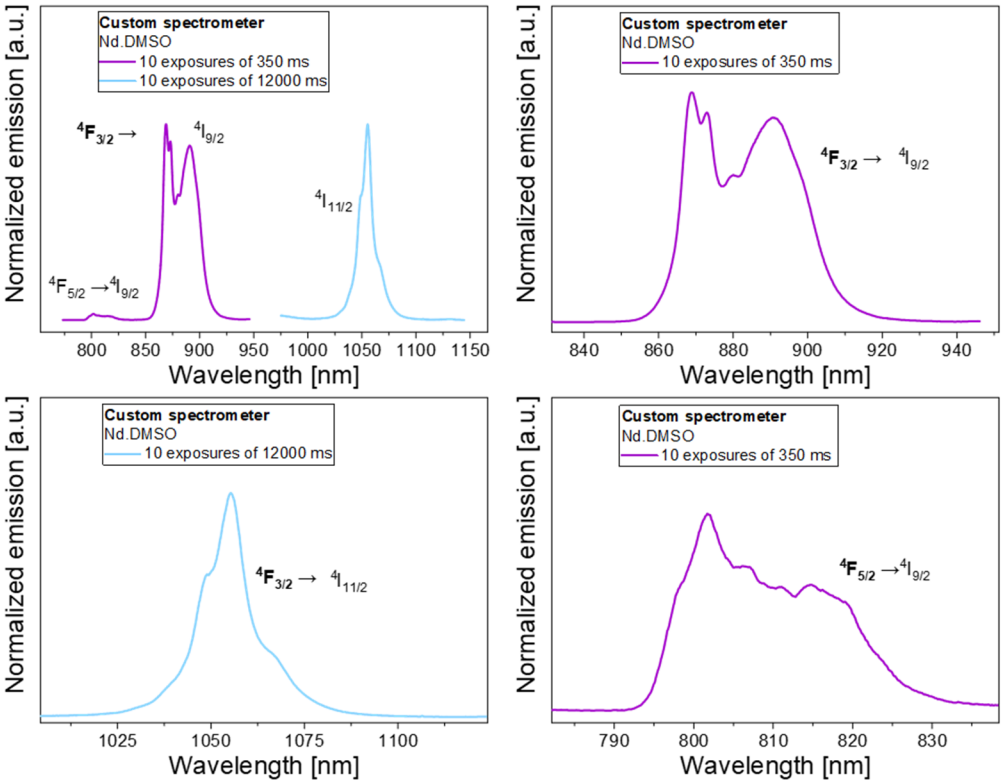

Figure 6 – Emission spectra of 50 mM neodymium(III) in DMSO recorded on the custom spectrometer using an excitation wavelength of 580 nm. Exposure times and number of exposures per measurement is changed to optimize for good signal-to-noise ratios.

4. Conclusion

We have built a custom spectrometer, and reported the methodologies to achieve intensity, wavelength, and integration time corrected emission spectra in the range from 450—950 nm. We have documented a spectral resolution of 0.6 nm, and shown that the custom spectrometer can record uncorrected spectra from 450—1150 nm. We are thus able to conclude that we in this report provide an unprecedented tool for studying lanthanide luminescence in solution.

The next steps are: 1) create a single software interface, instead of using four different pieces of software; 2) develop integration time calibration for long calibration times across difference gratings; 3) extend the range to include the lanthanide(III) ions that luminesce up to 2000 nm; 4) enable excitation source intensity calibrations and the measurements of excitation spectra; and 5) use the unprecedented capabilities of the spectrometer to explore new and exciting lanthanide chemistry.

Acknowledgements

The authors thank Carlsbergfondet, Villum Fonden (Grant No. 14922), the University of Copenhagen. We thank Magnus Christian Wied for software assistance during the spectrometer setup.

References

1. Z. Liao, M. Tropiano, K. Mantulnikovs, S. Faulkner, T. Vosch and T. Just Sørensen, *Chemical Communications*, 2015, **51**, 2372-2375.
2. Z. Liao, M. Tropiano, S. Faulkner, T. Vosch and T. J. Sørensen, *RSC advances*, 2015, **5**, 70282-70286.
3. P. R. Nawrocki, K. M. Jensen and T. J. Sørensen, *PCCP*, 2020, **22**, 12794-12805.
4. N. Kofod, P. Nawrocki and T. J. Sørensen, *The Journal of Physical Chemistry Letters*, 2022, **13**, 3096-3104.
5. N. Kofod, L. G. Nielsen and T. J. Sørensen, *The Journal of Physical Chemistry A*, 2021, **125**, 8347-8357.
6. M. H. V. Werts, R. T. F. Jukes and J. W. Verhoeven, *Physical Chemistry Chemical Physics*, 2002, **4**, 1542-1548.
7. V. Lavín, U. R. Rodríguez-Mendoza, I. R. Martín and V. D. Rodríguez, *Journal of Non-Crystalline Solids*, 2003, **319**, 200-216.
8. E. Moret, J.-C. G. Bünzli and K. J. Schenk, *J Inorganica Chimica Acta*, 1990, **178**, 83-88.
9. Y. Cai, Z. Wei, C. Song, C. Tang, W. Han and X. J. C. S. R. Dong, 2019, **48**, 22-37.
10. J. Zhao, D. Zhong and S. Zhou, *Journal of Materials Chemistry B*, 2018, **6**, 349-365.
11. S. Zhu, B. C. Yung, S. Chandra, G. Niu, A. L. Antaris and X. J. T. Chen, 2018, **8**, 4141.
12. J. Cao, B. Zhu, K. Zheng, S. He, L. Meng, J. Song, H. J. F. i. b. Yang and biotechnology, 2020, 487.
13. M. Blanco and I. Villarroya, *TrAC Trends in Analytical Chemistry*, 2002, **21**, 240-250.
14. S. A. Payne, J. A. Caird, L. Chase, L. K. Smith, N. D. Nielsen and W. F. J. J. B. Krupke, 1991, **8**, 726-740.
15. Y. Ozaki, *J Analytical Sciences*, 2012, **28**, 545-563.
16. R. Carr, R. Puckrin, B. K. McMahon, R. Pal, D. Parker and L.-O. Pålsson, *Methods and Applications in Fluorescence*, 2014, **2**, 024007.
17. R. Pal and A. Beeby, *Methods and Applications in Fluorescence*, 2014, **2**, 037001.
18. E. N. Ward and R. Pal, *Journal of Microscopy*, 2017, **266**, 221-228.
19. J. Kimball, J. Chavez, L. Ceresa, E. Kitchner, Z. Nurekeyev, H. Doan, M. Szabelski, J. Borejdo, I. Gryczynski and Z. Gryczynski, *Methods and Applications in Fluorescence*, 2020, **8**, 033002.
20. L. Ceresa, J. Kimball, J. Chavez, E. Kitchner, Z. Nurekeyev, H. Doan, J. Borejdo, I. Gryczynski and Z. Gryczynski, *Methods and Applications in Fluorescence*, 2021, **9**, 035005.
21. D. M. Jameson, J. C. Croney and P. D. J. Moens, in *Methods in Enzymology*, Academic Press, 2003, vol. 360, pp. 1-43.
22. C. Song, Y. Huang, Y. Yan, D. Cui, G. Wang, Y. Niu and B. Liu, 2021.
23. F. Leng and G. Nyberg, *Journal of Physics E: Scientific Instruments*, 1977, **10**, 686.
24. G. Xiong, J. Zhang, G. Yang, J. Yang, H. Li, Z. Hu, Y. Zhao, M. Wei and T. Yi, *Physica Scripta*, 2014, **89**, 065005.
25. E. B. Jochnowitz and J. P. Maier, *Molecular Physics*, 2008, **106**, 2093-2106.
26. A. Beeby and S. Faulkner, *Chemical Physics Letters*, 1997, **266**, 116-122.
27. N. Kofod, P. Nawrocki, C. Platas-Iglesias and T. J. Sørensen, *Inorganic Chemistry*, 2021.
28. Y. Hasegawa, M. Iwamuro, K. Murakoshi, Y. Wada, R. Arakawa, T. Yamanaka, N. Nakashima and S. J. B. o. t. C. S. o. J. Yanagida, 1998, **71**, 2573-2581.
29. K. Binnemans, *Coordination Chemistry Reviews*, 2015, **295**, 1-45.
30. N. Kofod, P. Nawrocki, M. Juelsholt, T. L. Christiansen, K. M. Ø. Jensen and T. J. Sørensen, *Inorganic Chemistry*, 2020, **59**, 10409-10421.
31. P. Babu and C. Jayasankar, *J Physica B: Condensed Matter*, 2000, **279**, 262-281.
32. X. Y. Chen and G. K. Liu, *Journal of Solid State Chemistry*, 2005, **178**, 419-428.
33. N. M. Shavaleev, S. V. Eliseeva, R. Scopelliti and J.-C. G. Bünzli, *Chemistry – A European Journal*, 2009, **15**, 10790-10802.
34. A. Døssing, A. Kadziola, P. Gawryszewska, A. Watras and A. J. I. C. A. Melchior, 2017, **467**, 93-98.
35. X. Zhou, C. S. Mak, P. A. Tanner and M. D. Faucher, *Physical Review B*, 2006, **73**, 075113.
36. B. S. Chong and E. G. J. I. c. Moore, 2018, **57**, 14062-14072.
37. A. D'aléo, A. Picot, A. Beeby, J. Gareth Williams, B. Le Guennic, C. Andraud and O. J. I. c. Maury, 2008, **47**, 10258-10268.
38. T. S. Lomheim and L. G. De Shazer, *Physical Review B*, 1979, **20**, 4343-4356.
39. Y. C. Ratnakaram and A. Viswanadha Reddy, *Journal of Non-Crystalline Solids*, 2000, **277**, 142-154.
40. K. Driesen, P. Nockemann and K. Binnemans, *Chemical Physics Letters*, 2004, **395**, 306-310.
41. P. R. Nawrocki, N. Kofod, M. Juelsholt, K. M. Ø. Jensen and T. J. Sørensen, *Physical Chemistry Chemical Physics*, 2020, **22**, 12794-12805.

42. L. G. Nielsen and T. J. Sørensen, *Inorganic Chemistry*, 2019, DOI: 10.1021/acs.inorgchem.9b01571.
43. N. Kofod, P. Nawrocki, M. Juelsholt, T. L. Christiansen, K. M. Ø. Jensen and T. J. Sørensen, *Inorganic Chemistry*, 2020, **59**, 10409-10421.
44. L. G. Nielsen, A. K. R. Junker and T. J. Sørensen, *Dalton Transactions*, 2018, **47**, 10360-10376.

Placeholder TOC photo: